European Journal of Environmental and Civil Engineering

ISSN: (Print) (Online) Journal homepage: https://www.tandfonline.com/loi/tece20

Effects of blending manufactured sand and offshore sand on rheological, mechanical and durability characterization of lime-cement masonry mortar

Branavan Arulmoly, Chaminda Konthesingha & Anura Nanayakkara

To cite this article: Branavan Arulmoly, Chaminda Konthesingha & Anura Nanayakkara (2021): Effects of blending manufactured sand and offshore sand on rheological, mechanical and durability characterization of lime-cement masonry mortar, European Journal of Environmental and Civil Engineering, DOI: 10.1080/19648189.2021.1995506

To link to this article: https://doi.org/10.1080/19648189.2021.1995506

Published online: 08 Nov 2021.

EUROPEAN JOURNAL OF ENVIRONMENTAL AND CIVIL ENGINEERING
https://doi.org/10.1080/19648189.2021.1995506

Effects of blending manufactured sand and offshore sand on rheological, mechanical and durability characterization of lime-cement masonry mortar

Branavan Arulmoly[a], Chaminda Konthesingha[a] and Anura Nanayakkara[b]

[a]Department of Civil Engineering, University of Sri Jayewardenepura, Ratmalana, Western Province, Sri Lanka;
[b]Department of Civil Engineering, University of Moratuwa, Moratuwa, Western Province, Sri Lanka

ABSTRACT

The environment and ecological systems are suspected of serious drawbacks as a result of the over-extraction of river sand for construction activities. An attempt was made in this research on completely replacing river sand in lime-cement masonry mortars with blended sands comprised of manufactured sand and offshore sand. The S and N types (as defined in the standards) were selected for producing masonry mortars with different sand contents. For each type, five mortars were prepared to contain river sand alone (reference mortar), manufactured sand alone, and three blended sands (replacing manufactured sand by offshore sand at 25%, 50%, and 75%). Because of the dominant roles of particle angularity, surface roughness, and gradation of the alternatives, the performance of mortars was evaluated and compared based on these sand characteristics. Furthermore, the level of statistical significance of the experiment results was analyzed from a single factor one-way ANOVA test. Outcomes of this research revealed that the blended sands and manufactured sand declined the fresh state performance of mortars than the river sand mortars. However, most of the stiffened and durability properties of alternative mortars were significantly advanced than the reference mortars.

ARTICLE HISTORY
Received 5 June 2021
Accepted 13 October 2021

KEYWORDS
Fine aggregate; river sand; mortar; angularity; surface roughness; mechanical characterization

1. Introduction

Mortar plays a crucial role in masonry constructions which is the most utilized cement-based composite material next to concrete (Cuffari, 2019; Jaffe, 2001). The current situation has become more complicated to achieve the need for an enlargement of existing infrastructures. The evolution of infrastructure developments leads the construction industries to acquire more naturally available resources for producing mortars (Padmalal et al., 2008). Fine aggregate solely influences the performance of fresh and hardened mortar, when it is bound with the cement paste (Branavan et al., 2020; Arulmoly et al., 2021). The recent survey carried out by Branavan and Konthesingha (2019) in 2019 revealed that more than 90% of the local construction works are still being operated with river sand (RS) as the primary fine aggregate, which evinced serious environmental issues and the inflated demand (Gavriletea, 2017; Koehnken et al., 2020; Pereira & Ratnayake, 2013).

Few studies have demonstrated the possibilities of using manufactured sand (MS) and offshore sand (OS) as the alternatives for partially replacing RS in mortars. Gonçalves et al. (2007) evaluated the performance of mortars with MS produced from different crushers (such as cone and impact crushers) and compared it with the RS mortars. Authors identified that the impact crushed MS mortar revealed higher

CONTACT Branavan Arulmoly brana14arul@gmail.com Department of Civil Engineering, University of Sri Jayewardenepura, Ratmalana, 10340, Western Province, Sri Lanka.

Table 1. Properties of PLC complying with EN 197-1 (British Standards Institution, 2000).

Property	PLC	Standard limits
Compressive strength (2 days)	>27 N/mm^2	≥ 20 N/mm^2
Compressive strength (28 days)	>50 N/mm^2	42.5–62.5 N/mm^2
Initial setting time	130–150 min	≥ 60 min
Blaine fineness	370–390 m^2/kg	Not defined
Soundness	<1 mm	≤ 10 mm
Loss of ignition	$<8\%$	Not defined
Sulfate content (SO_3)	$<3\%$	$\leq 4.5\%$
Chloride content	$<0.08\%$	$\leq 0.1\%$
Loss of ignition (LOI)	$<3\%$	Not defined
Insoluble residue (IR)	$<3\%$	$<5\%$

packing density which resulted in reduced porosity, lower absorptivity, and higher compressive strength than reference mortars. Bederina et al. (2013) observed an improved durability performance of limestone MS mortar against the hydrochloric acid and lime solutions than RS mortar. Furthermore, Radhakrishna & Kumar, 2018) reported increased compressive strength and elastic modulus of MS mortar when RS was substituted in the range of 40%–60%. Balasubramanian et al. (2016) also identified inflated compressive and split tensile strengths of MS mortar than RS mortar. Aoual-Benslafa et al. (2015) studied the durability of mortars made with dredged sand. Authors concluded that the replacement of RS with dredged sand exhibited lower compressive strengths and advanced the durability against hydrochloric acid and hydrogen sulfate solutions.

Some studies have presented the material properties of different fine aggregates and their impact on the performance of concrete. Alshibli and Alsaleh (2004) correlated the surface roughness and shape of three silica sand from digital microscopy and the friction and dilatancy angles. Authors identified that the increased angles with higher roughness of particles significantly influenced the concrete hardened properties. Li et al. (2011) reported that the higher surface roughness of MS particles considerably improved the compressive strength, flexural strength, and abrasion resistance of pavement cement concrete. Some contradictory results were noticed in the study made by Shen et al. (2016) where the authors demonstrated higher strengths of concrete with lower angularity and surface roughness of MS. Moreover, Poloju et al. (2017) reported that the shape and texture indexes were reduced when RS was replaced with stone dust. This demonstrated decreased compressive strength and workability and the increased split tensile strength of concrete.

Based on a brief review, it was observed that the past studies were executed replacing RS with either MS or OS in mortars. Some studies are reporting the effects of aggregate properties on the performance of concrete. However, the characteristics of fresh and hardened mortars may also be significantly affected by the sand properties due to the absence of coarse aggregates (Branavan & Chaminda, 2021). Therefore, this study aims to check the efficacy of blending MS and OS for a complete replacement of RS in lime-cement mortars.

2. Research significance

To immediately cease the problems with over-extraction of RS, a novel concept was introduced in this study concerning the blending of MS with OS at different replacement levels for lime-cement masonry mortar. This can be considered as an effective solution for completely replacing RS, which is beneficial in producing sustainable masonry mortars (Arulmoly et al., 2021). Most of the available standards report the usage of either siliceous sand or crushed sand in mortars. However, the blending of both sand types for masonry mortars is mentioned in none of the standards.

MS can be considered as one of the emerging solutions for replacing RS due to the availability of rock sources for production (Chow et al., 2013; Wigum et al., 2009; Arulmoly et al., 2021). OS is also abundantly available, which is dredged from the deep-sea beds and processed to achieve compliance for use as a fine aggregate in cement-based mixes (Dias et al., 2008; Limeir et al., 2013). Because of the varying sources and processing techniques, the MS and OS particles are differed mainly based on physical characteristics such as angularity and surface roughness. The blending of both could resolve the issues when they are individually incorporated in mortars. Hence, this is also elaborated in this study by analyzing the

Figure 1. Selected fine aggregates for the study.

effects of combined particle physical properties of blended sands on the rheological, mechanical, and durability properties of masonry mortars which is not executed by the past studies.

3. Materials and methods

3.1. Materials

A Portland Limestone Cement (PLC) classified under the CEM II/A-LL 42.5 R of EN 197-1 (British Standards Institution, 2000) was utilized as the primary binding material. Table 1 lists the technical specifications of PLC and the compliance with the corresponding standard. A hydrated lime (HL) conforming to ASTM C207 (ASTM International, 2018b) was used as the mineral admixture in this study, which was classified as the '*Type 1: Dolomitic Lime*' as specified by ICTAD SCA/4/I (ICTAD, 2004) and '*CL 90 S*' according to EN 459-1 (British Standards Institution, 2015) based on the purity (i.e., the mass of CaO + MgO is 93.23%). These binding materials were selected based on the widespread usage by the local contractors in Sri Lanka these days.

Three types of fine aggregates as shown in Figure 1 were utilized for this study. RS was directly extracted from a riverbed located in Mahiyanganaya area (Uva province) for producing the reference mortars. MS was obtained from a crushing plant located in Unawatuna area (Southern province). It should be noted that the rock source used to produce MS was '*Charnockite*' which can be classified as a high-grade metamorphic rock. OS was extracted from an open stockpile located in Muthurajawela area (Western province).

Table 2 shows the chemical properties of the constituents of mortars obtained through the XRF technique. As provided, each selected sand can be classified as the '*Siliceous material*' which showed more than 70% of silica. In addition, considerable percentages of Al_2O_3, Fe_2O_3, and CaO were also detected. Table 3 represents the mineralogical compositions of the selected fine aggregates which were identified from the XRD test method. Since the source for the production of MS is Charnockite, was highly detected quartz, albite, and K-feldspar. RS and OS highly contained quartz as similar to MS which comply with the silicate aggregates. In addition, a few contents of calcite, K-feldspar, and hematite were also observed. When comparing the provision given in the standard ASTM C294 (ASTM International, 2019b), all the minerals that were detected in the sand types selected are falling in the category of 'affable minerals'. This clearly defines the risk-free usage in cement-based mixes. Some potential minerals such as illite and biotite were also observed in very small quantities.

3.2. Characterization of fine aggregates

Table 4 tabulates the physical properties of the selected fine aggregates which were investigated at the early stage of this study. Because of the tolerable presence of potentially harmful minerals such as clay and silt, the RS was directly incorporated in the mortars without any pre-preparations. Regarding the deleterious contents in OS, the chloride content satisfied with the maximum permissible limitations provided by the standards such as 0.1%–0.4% by BS 5328 (British Standards Institution, 1997) and 0.1% by

Table 2. Chemical properties of the constituents (%).

	SiO_2	Al_2O_3	Fe_2O_3	CaO	MgO	SO_3	Na_2O	K_2O	CO_2
RS	97.53	2.84	0.19	0.00	0.00	0.00	0.00	0.76	—
MS	72.01	7.83	2.09	3.95	0.25	0.00	2.08	2.54	—
OS	65.84	15.24	4.78	2.55	2.09	0.00	0.00	0.00	—
Hydrated lime	0.35	0.13	0.07	88.91	4.32	—	—	—	2.01
PLC	C_3S	C_2S	C_3A	C_4AF	MgO	SO_3	LOI	CaO	
	51.34	23.68	6.41	11.82	2.90	2.50	0.76	1.07	

Table 3. Mineralogical properties of the fine aggregates (%).

	Calcite	Quartz	Albite	K-Feldspar	Magnetite	Anorthite	Dolomite	Illite	Biotite	Hematite	Kyanite	Aragonite
RS	7.99	35.69	3.26	5.11	0.07	0.98	0.00	0.95	0.00	0.79	0.00	0.03
MS	18.97	27.95	18.03	27.15	0.32	4.36	0.23	1.66	0.00	0.11	0.00	0.00
OS	8.41	31.59	8.49	13.68	6.51	1.05	1.54	0.61	0.00	3.66	0.84	0.00

Table 4. Physical properties of fine aggregates and the standards referred.

Property	RS	MS	OS	Standard
Specific gravity	2.64	2.70	2.67	ASTM C128 (ASTM International, 2001)
Fineness modulus	3.113	3.086	2.128	ASTM C144 (ASTM International, 2018a)
Water absorption (%)	0.95	1.1	0.75	ASTM C70 (ASTM International, 2006)
Void content (%)	38.143	39.167	38.256	ASTM C29 (ASTM International, 1997)
Surface moisture (%)	1.675	2.371	2.427	ASTM C70 (ASTM International, 2006)
Micro fines (<0.075 mm) (%)	0.18	3.37	0.24	ASTM C117 (ASTM International, 1995)
Clay content (%)	1.59	0.39	1.18	ASTM C142 (ASTM International, 2010)
Silt (%)	0.29	1.92	0.95	—
Chloride (%)	—	—	0.086	—
Salt (%)	0.0039	—	0.016	—
Shells (%)	—	—	7.45	—

BS EN 998-2 (British Standards Institution, 2016). The salt and sulfate contents of OS were also identified in small quantities. Furthermore, the study implemented by Dias et al. (2008) highlighted the possibility of utilizing OS in concrete from the same stockpile selected for this study. Therefore, the durability studies on mortars incorporated OS were not executed in this study.

The MS was produced in the crushing plants through several processing stages. Vertical shaft impactors at different levels were used to reduce the particle sizes to the desired ranges to achieve the requirement. After the crushing and screening of particles, the material was washed to remove the excess micro fines and then stored for future use. As provided, it can be observed that the micro-fine content of MS after washing was 3.37%, which satisfied the permissible limit of 16% as provided by BS 882 (British Standards Institution, 1992).

The sections below describe the properties of fine aggregates which highly influenced the performance of lime-cement masonry mortars. Three different blended sand were incorporated in the mortars by replacing 25% (B3), 50% (B2), and 75% (B1) of MS by OS (by weight basis).

3.2.1. Particle size distribution and packing density

The gradation test was carried out for each selected fine aggregate and the blended sands according to ASTM C144 (ASTM International, 2018a). RS substantially lied within the allowable region suggested by the standard which revealed a uniform particle size distribution. However, MS and OS did not comply with the limitations for some particle size ranges. The corresponding gradation curves are illustrated in Figure 2. It can be identified that the MS particles greater than 2.36 mm and the OS particles in the range of 0.65–1.18 mm lied out of the tolerable zone.

Fine aggregate should have a required particle size distribution before applying in cement-based mixes. This is to ensure the minimum requirement of cement, better particle interlocking, and reduction of void content. With respect to the results mentioned above, the selected MS and OS cannot be directly applied to mortar as they are not conforming to the standard gradation limits according to ASTM C144 (ASTM International, 2018a). However, the blending of both alternatives at each selected level resolved

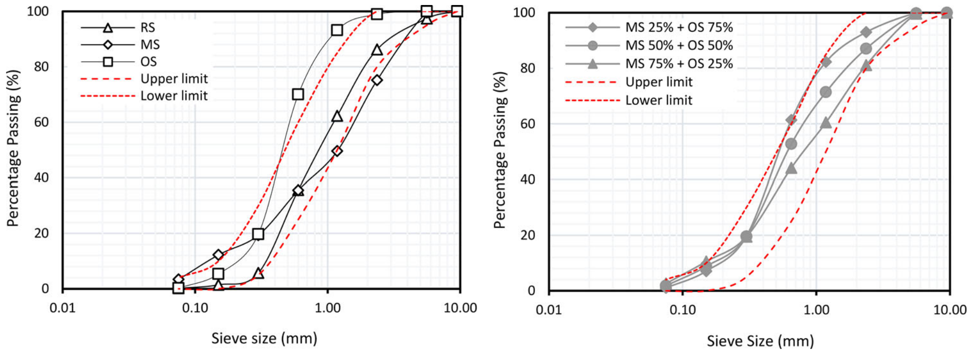

Figure 2. Gradation curves conforming to ASTM C144 (ASTM International, 2018a) for particles above 0.075 mm (primary fine aggregates—left; blended sands—right).

this issue. When the MS content in the blended sand changed from 25% to 75%, the gradation curve was shifted from left to right. Also, allgradation curves of the blended sands lied within the required region. Therefore, these blended sands can be directly applied to mortar.

The particle size distribution of fine aggregates may significantly affect their density. To numerically study these effects, the packing density of the selected fine aggregates and blended sands were investigated from a rodding testing method based on ASTM C29 (ASTM International, 1997). As provided in Figure 3, among the selected fine aggregates MS revealed the highest packing density. This shows a contradictory relation when correlating with the particle size distribution. Here, the presence of higher microfine in MS considerably increased the overall density than RS and OS. Regarding the blended sands, it can be distinctly observed that the packing density was advanced linearly with the reducing replacement levels. This was due to the increasing contribution of MS.

3.2.2. Angularity

From the previous studies, the more angularity of MS contributes both merits and demerits to the cement-based mix performance. This section describes the actual shapes of RS, MS, and OS particles considered in this study and their combined effects in the blended sands. Here, the shapes of particles were initially observed through optical microscopy. For this analysis, representative samples were selected from each sand type and then washed and oven-dried to remove any impurities that were attached to the sand surfaces. This was done to ensure the actual characteristics of particles without the influence of other impurities. After the pre-preparation works, sand particles were observed through an optical microscope, and initially, the corresponding gray-scale micro images of sand particles were produced. After that, these images were processed through the '*ImageJ*' software to produce the threshold b/w images (refer Figure 4) to observe the shape characteristics.

MS particles were detected with more angular or cubical shapes than the RS and OS particles. Considering Figure 4(b), sharp tips and straight edges can be observed with MS which shows more angularity. Contrast characteristics were noticed with RS and OS (see Figure 4 (a,c)) where the particles reveal round edges instead of sharp edges. This manifests the less angularity/round RS and OS than MS.

To check the accuracy of the qualitative analysis on the angularity of particles, a quantitative technique suggested by Murdock (Murdock, 1960) was referred to numerically investigate the shape characteristics using an index method. Here, the angularity index (f_A) was determined for each fine aggregate as well as the blended sand using Equation (1), which is based on the identification of the voids present in the sand sample after sufficient compaction.

$$f_A = (3 \times f_H)/20 + 1 \quad (1)$$

Here, $f_H = 67 - (M_s \times 100)/(M_w \times G_s)$; M_s = mass of sand after compaction; M_w = mass of water to fill the container; G_s = specific gravity of sand.

The f_A varies from 0 to 11 can be considered as the fine aggregate and applied to the cement-based mixes. Also, the more f_A of sand represents the more angularity of particles. Concerning the index values all fine aggregates and blended sand complied with the above requirement. MS manifested the highest

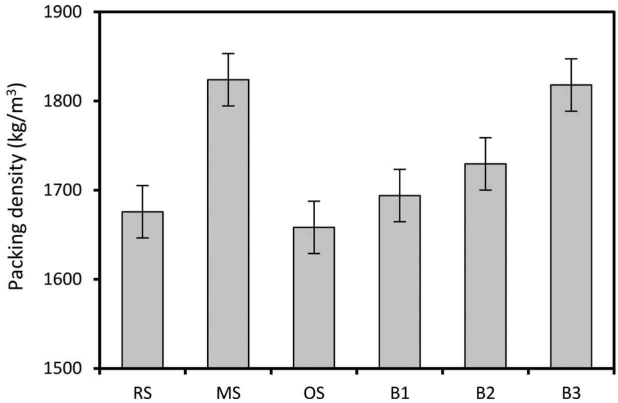

Figure 3. Packing density of fine aggregates and blended sands.

index which highlights the cubical shape of particles. RS and OS were arrived with low indexes and this represents the roundness of the particles. All the angularity indexes of blended sands lied between RS and MS. Figure 5 can be referred for comparing the angularity index of each sand type which was determined using the above method.

3.2.3. Surface roughness

As represented in Figure 4, the image processing was also carried out to visually inspect the surface roughness of the sand types after all the pre-preparation works as described under Section 3.2.2. Here, the different color shades highlight the different phases of the surfaces (Note that the identification of different phases was done using a threshold process which was executed at the same observation angle for each sand type). During the thresholding of gray-scale images, red, black, and gray shades were noticed in most of the MS particles, and this manifests the higher number of phases and thus the increased roughness. However, only two phases were identified in the RS and OS particles which reveals more smoothness of the particles than MS.

As similar to the angularity, here also a quantitative test was done to compare the surface roughness using a standard test procedure recommended by ASTM D3398 (ASTM International, 2000b). The surface roughness index (f_I) was determined for each fine aggregate and blended sand using Equation (2). This method also relies on the voids presented in different size fractions of the sand samples after the required compactions.

$$f_I = (P \times I_a) + 100 \tag{2}$$

Here, $I_a = 1.25 \times V_{10} - 0.25 \times V_{50} - 32$; P = passing percentage of the size fraction; V_{10} = void content after 10 drops per layer; V_{50} = void content after 50 drops per layer.

Figure 6 shows the mean of the weighted surface roughness index of the individual size fractions determined from the above method for each fine aggregate and blended sand. It can be observed that as similar to the threshold microimages the MS particles arrived with the maximum index which highlights the rougher surface particles. Moreover, the OS and blended sands revealed slightly higher indexes than RS.

3.3. Mix design of mortars

Conventional mix design was followed up in this study for designing the mortar mixes. The consumption of fine aggregates in mortars was done based on saturated surface dry (SSD) conditions. The lime:cement:sand (L:C:S) ratios which are the most commonly used in the masonry practices in Sri Lanka were selected for casting the mortars in this study. The standard specifications such as ASTM C270 (ASTM International, 2019a) and ICTAD SCA/4/I (ICTAD, 2004) were also used as supportive documents in selecting the mixing ratios. Totally 10 mortars were cast in this study and Table 5 tabulates the selected mixing ratios and the quantities of each constituent with initial water to cement ratio of 0.5. The mortars were

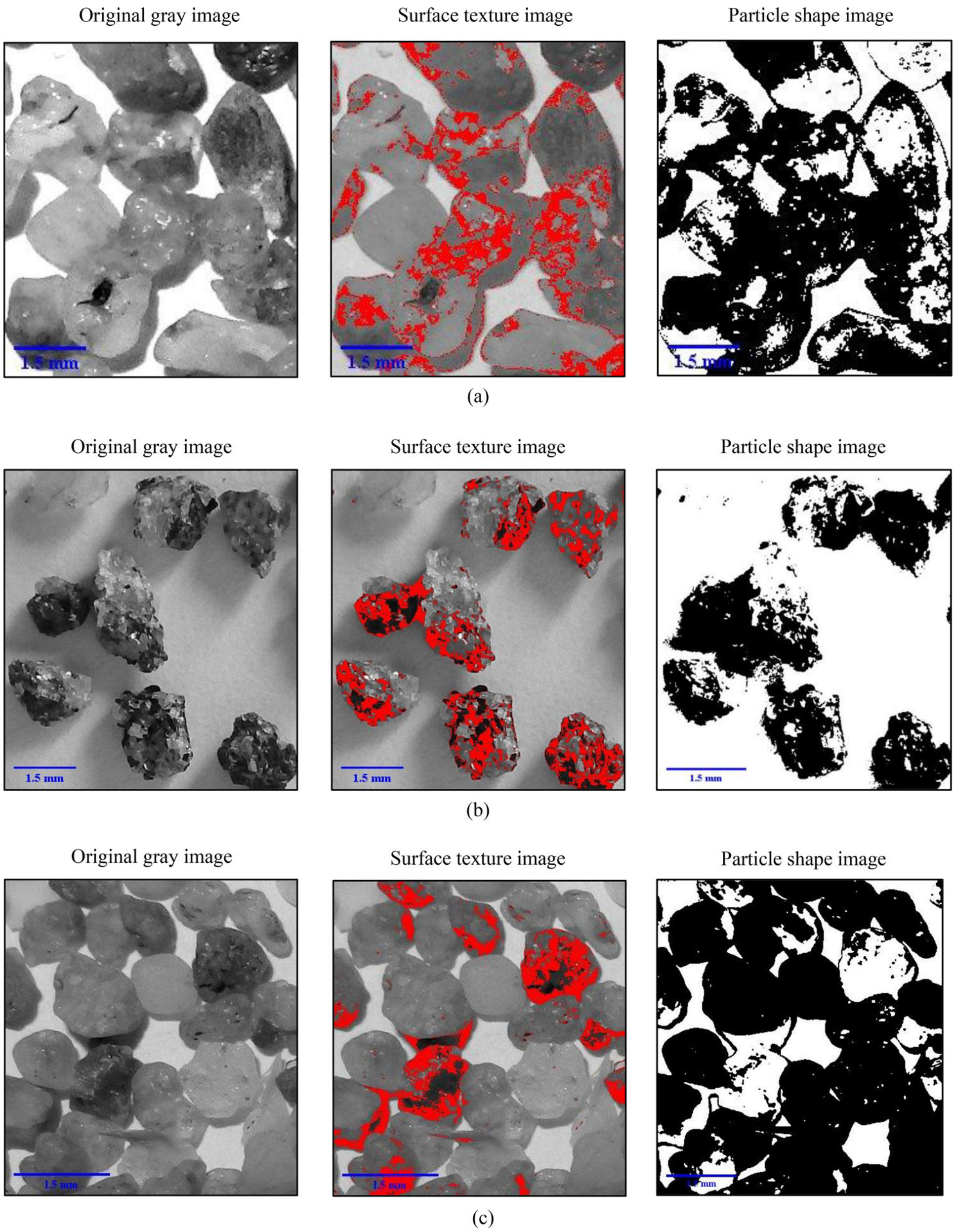

Figure 4. Surface textures and shapes of particles in the range of 1.4 – 2.8 mm (a) RS particles; (b) MS particles; (c) OS particles.

mixed using a mechanical mortar mixer at a temperature of 25 ± 2 °C. Here, mortars incorporated RS alone were considered as the reference mortars and the alternate mortars were compared with the reference mortars during the analysis.

3.4. Test methods

The fresh and hardened state properties of mortars were evaluated in this study to check the effects of different sand inclusions. The laboratory experiments were carried out using ASTM and EN standards. Table 6 lists down the test methods, standards referred, the number of samples prepared for each test, the climatic conditions maintained, and the selected curing periods. It should be also noted that a

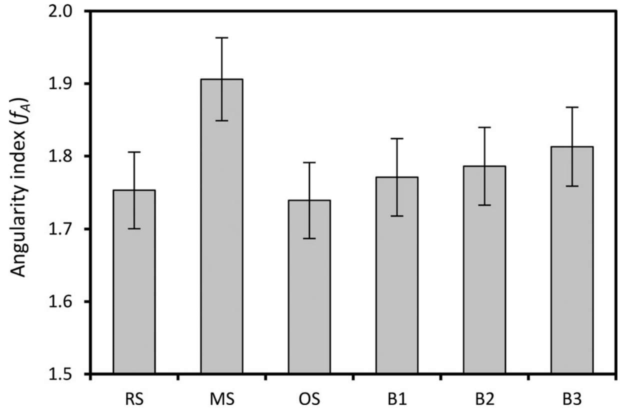

Figure 5. Angularity index of fine aggregates and blended sands.

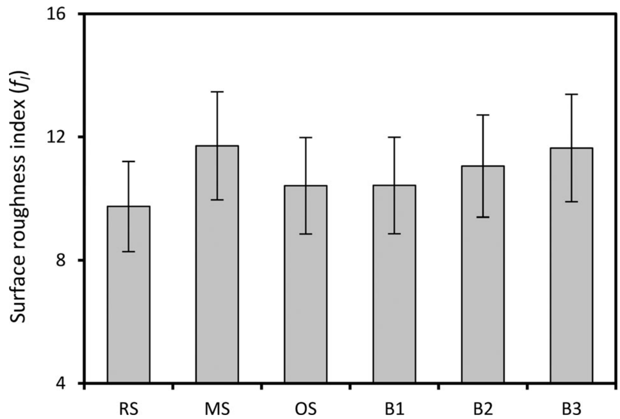

Figure 6. Surface roughness index of fine aggregates and blended sands.

Table 5. Mortar constituents.

Type	Designation	L:C:S	HL (kg/m^3)	PLC (kg/m^3)	RS (kg/m^3)	MS (kg/m^3)	OS (kg/m^3)	Water (kg/m^3)	Density (kg/m^3) Wet	Density (kg/m^3) Dry	w/c_{ef}
S mortar	1-RS	0.5:1:4.5	186	525	1976				2292	2047	0.48
	2-MS					2021			2396	2098	0.59
	3-B1					505	1499	263	2301	2058	0.45
	4-B2					1010	999		2316	2074	0.51
	5-B3					1516	500		2338	2084	0.55
N mortar	6-RS	1:1:6	279	394	1976				2255	1825	0.49
	7-MS					2021			2341	2024	0.61
	8-B1					505	1499	197	2269	1898	0.46
	9-B2					1010	999		2275	1945	0.53
	10-B3					1516	500		2281	2003	0.58

standard jolting apparatus was used to provide compaction for mortar samples prepared for the hardened properties tests. After the required compaction, the samples were stored inside polyethylene covers and kept undisturbed for 24 hours. A ponding method was used for curing the mortar specimens after being removed from the moulds.

The fresh tests were executed on the mortars just after the mixing. The wet bulk density was determined initially using a vibration method as illustrated in EN 1015-6 (British Standards Institution, 2007a). Then the workability was evaluated with a standard flow table test method and the consistency was measured using a standard plunger penetration method. Another standard needle penetration method as described in EN 1015-9 (British Standards Institution, 1999b) was referred to investigate the workable

Table 6. Experimental plan and standards referred.

	Property	No of specimens	Climatic condition	Curing age (days)	Standard
Fresh	Wet bulk density	2	T: 25 ± 2 °C	—	EN 1015-6 (British Standards Institution, 2007a)
	Workability	2	T: 25 ± 2 °C	—	EN 1015-3 (British Standards Institution, 2004)
	Consistency	2	T: 25 ± 2 °C	—	EN 1015-4 (British Standards Institution, 1999a)
	Workable life	2	T: 20 ± 2 °C, RH: 95%	—	EN 1015-9 (British Standards Institution, 1999b)
	Bleeding	2	T: 23 ± 2 °C, RH: 95%	—	ASTM C940 (ASTM International, 2003)
	Water retentivity	2	T: 23 ± 2 °C, RH: 95%	—	ASTM C1506 (ASTM International, 2017)
Hardened	Dry bulk density	3	T: 105 ± 5 °C	1	EN 1015-10 (British Standards Institution, 2007b)
	Compressive strength	6	T: 20 ± 2 °C, RH: 65% ± 5%	2, 28	EN 1015-11 (British Standards Institution, 2007c)
	Flexural strength	3	T: 20 ± 2 °C, RH: 65% ± 5%	2, 28	EN 1015-11 (British Standards Institution, 2007c)
	Linear shrinkage	4	T: 23 ± 2 °C, RH: 62% ± 5%	56	ASTM C531 (ASTM International, 2000a)
	Thermal expansion	4	T: 100 ± 2 °C	28	ASTM C531 (ASTM International, 2000a)
	Capillary water absorption	4	T: 24 ± 8 °C, RH: 60% ± 5%	28	ASTM C1403 (ASTM International, 2013)
Durability	Alkali-Silica reactivity	3	T: 80 ± 5 °C	56	ASTM C1260 (ASTM International, 2021)

Note. T = temperature; RH = relative humidity.

Table 7. Specimen types and dimensions for hardened and durability mortar tests.

Test	Dry bulk density, flexural strength	Compressive strength	Linear shrinkage, thermal expansion & Alkali-silica reactivity	Capillary water absorption
Type	Prism	Half-prism	Auto-clave bar	Cube
Specimen	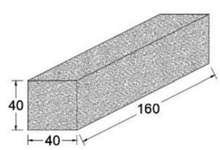	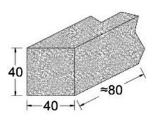	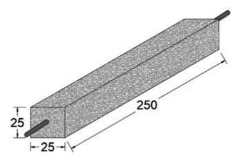	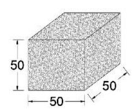
Size (mm)	40 × 40 × 160	40 × 40 × 80	25 × 25 × 250	50 × 50 × 50

life of mortars. Here, the workable life was determined when the mortars provided a penetration resistance of 0.5 N/mm^2. Some experimental setups were prepared for analyzing the bleeding and water retentivity of mortars. During the bleeding test, the accumulated water was extracted at prescribed intervals up to 1 hour period and the cumulative bleeding was calculated. The fresh mortars were subjected to a continuous suction for a 60 second period and the water retention capacity was calculated based on the difference of the flow of mortars before and after the suction.

The hardened properties of mortars were tested after the required curing ages. Table 7 illustrates the types of specimens prepared for the hardened state tests. The dry bulk density test was executed on mortar prism specimens which were stored in a laboratory oven at an elevated temperature for 24 hours. A universal testing machine was used to test the samples prepared for the determination of flexural and compressive strengths after 2 and 28 days of curing. Here, prism specimens were prepared for the flexural strength analysis, and the two parts resulted from the flexural test were tested for compressive strength. The flexural and compression loading was done on the specimen surfaces which were contacted with the moulds during the casting.

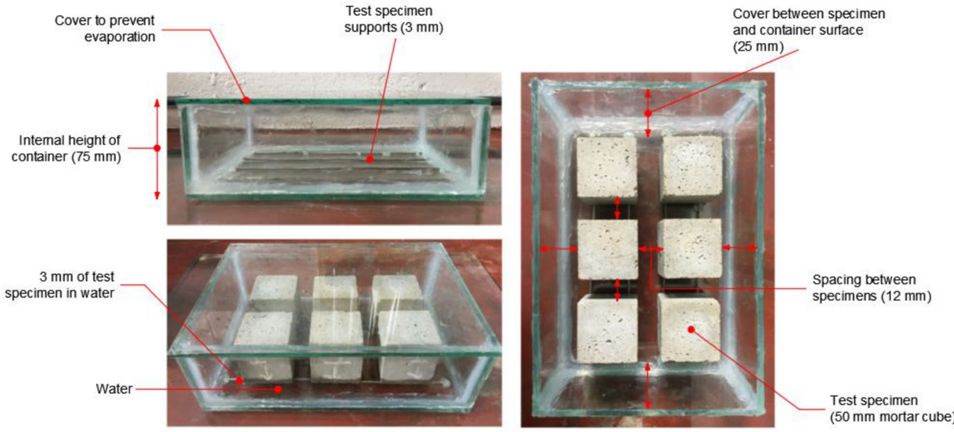

Figure 7. Setup for capillary water suction test and the specimen arrangements inside the uptake container according to ASTM C1403 (ASTM International, 2013).

For the investigation of linear shrinkage and thermal expansion of mortars, the auto-clave bars were provided with studs at both ends to measure the length change using a standard-length comparator. The linear shrinkage of mortars was evaluated up to 56 days from casting. During this curing period, the mortar bars were stored in a climatic chamber to attain the required environmental conditions. After the analysis, the mortar bars were undergone for repeat heating and cooling cycles until the bars achieved a constant length to eliminate the effect of shrinkage on the thermal expansion. The same length comparator was also used here to measure the length change after the mortar bars were stored at an elevated temperature.

A test setup as shown in Figure 7 was prepared for investigating the water absorption of mortars through the capillary pores. At the earlier stage of this experiment, the mortar cubes were stored inside moisture polyethylene bags for 28 days and then stored in a ventilated oven at $110 \pm 5\,°C$ for 24 hours. Before starting the test, specimens were cooled down for at least 2–3 hours to achieve the required temperature. All the other testing procedures were followed according to ASTM C1403 (ASTM International, 2013).

Since all the selected fine aggregates are silicate-based materials. A durability property of the selected mortars was investigated from the alkali-silica reactivity test as per ASTM C1260 (ASTM International, 2021). The corresponding specimen type used for this study is mentioned in Table 7. The mortar bars were prepared after the casting and cured for 24 hours inside a moist polyethylene cover. For the measurements, the length change apparatus used for the linear shrinkage and thermal expansion was also used. After the required curing, the mortar bars were then fully immersed in an airtight container filled with tap water and kept inside a cabinet at a temperature of 80 ± 5^{0}C for 24 hours. The initial length reading of each bar was then taken using the length comparator (with an accuracy of 0.001 mm) and recorded. Once all the recordings were done, the mortar bars were fully immersed inside an airtight container filled with 1 N NaOH solution, and the same temperature was maintained. The length changes attained by the mortar bars during the exposure to the NaOH solution were calculated at 3, 7, 14, 21, 28, and 56 days.

3.5. Method of analysis

A single factor one-way analysis of variance (ANOVA) was conducted to determine whether the selected alternatives and the blended sands had a statistically significant effect on the fresh and hardened properties of mortars. ANOVA was tested among each independent mortar which contained different sand contents for each type selected (S and N). Initially, a null hypothesis was set as '*no significant effects of the RS replacement on the property of mortar*' and the existence of the null hypothesis was checked at a 95% confidence interval. Therefore, when the *p*-value of ANOVA was less than 0.05, the null hypothesis was rejected.

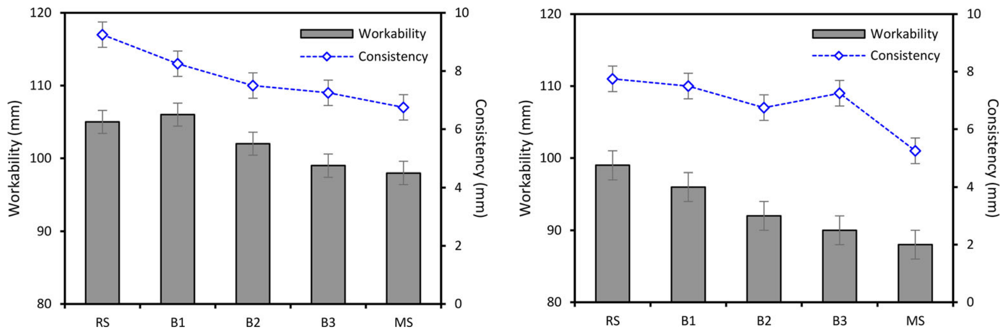

Figure 8. Effects of alternatives and blended sands on workability and consistency of S mortars (left) and N mortars (right).

Moreover, the effects of sand characteristics on the properties of mortars were evaluated using regression analysis by plotting linear or non-linear graphs concerning the mortar property and the corresponding sand characteristic. The trendlines were provided to identify whether the effects are increasing or decreasing.

4. Results and discussion

This section reports the effects of selected alternatives and blending ratios on the fresh and hardened state properties of lime-cement masonry mortars. During the analysis, all the properties of mortars were correlated with each characteristic of sands considered such as the packing density, angularity, and surface roughness. However, this article only includes the relationships identified with a high coefficient of determination (R^2) values.

4.1. Effects of blended sands on the properties of mortars

4.1.1. Wet and dry bulk densities

The mean wet and dry bulk densities of S and N mortars are tabulated in Table 5. Because the *p*-value of ANOVA was less than 0.05 (*p*-value = 6.1E-08), the complete replacement of RS with MS and the blended sands showed statistically significant effects on the mean wet bulk density of S mortars at a 95% confidence interval. Regarding the N mortars, the *p*-value of ANOVA was identified as 1E-07 which also revealed a statistically significant effect.

Regarding the mean dry bulk density of mortars, ANOVA resulted in the *p*-values for S and N mortars as 1.6E-08 and 5E-10, respectively. This also showed the statistically significant effects of RS replacements on the mean dry bulk density at a 95% confidence interval.

Here, it should be noted that the mean bulk density of mortars was significantly affected mainly due to the considerable deviations in the specific gravity of the selected sand types. As mentioned in Table 4, the specific gravity was increased as RS < OS < MS, which proved the high mean wet bulk density of MS and B3 mortars due to the increased MS content. A similar relationship can be found in the research by Aboutaleb et al. (2017), Samiei et al. (2015), and Safi et al. (2013) which were carried out with refractory bricks and plastic wastes, respectively. The authors found high bulk densities of mortars that contained the RS alternatives with larger relative density.

However, some studies suggested different properties that may also influence the wet bulk density of mortars. For example, Ledesma et al. (2014) and Neno et al. (2013) in their studies stated that the more fines content in recycled concrete and ceramic aggregates slightly lowered the bulk density than RS. Hence, from these conclusions, it can be also assumed that the higher microfine in MS contributed to the increased density of mortars.

4.1.2. Workability and consistency

The workability and consistency are considered the most important fresh properties of masonry mortar. The effects of RS replacement in mortars with the selected alternatives and blended ratios are graphically

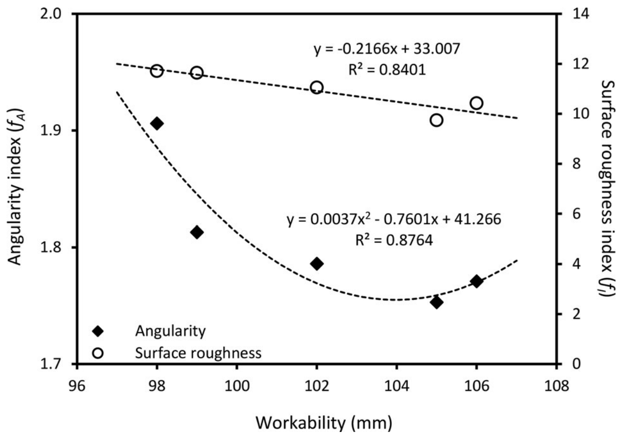

Figure 9. Relationships between workability of mortars and the particle indexes.

shown in Figure 8. As provided, the mean workability and consistency of mortars were linearly declined with the increasing MS contents. It should be also noted that the replacements of MS with OS in the blended sands also did not show an improved performance than RS mortars.

Furthermore, when considering the statistical approach on the workability of mortars, the *p*-value of ANOVA arrived as 0.00015 and 0.00013 for S and N mortars, respectively. Because the *p*-values were less than 0.05, the RS replacements with MS and blended sands had a statistically significant effect on the workability of S and N mortars at a 95% confidence interval. In addition, the selected replacements also had a statistically significant effect on the consistency of S and N mortars at 95% confidence interval as the *p*-values of ANOVA were obtained as 0.003 and 0.002, respectively.

The workability is simply termed as the flowability of mortars. The flow of mortars primarily depends on the lubricating effects created between the particles and cement paste (Gonçalves et al., 2007). Here, the rolling effects of sand particles act a vital role in providing the required lubricating effects to the mortars during the liquid phase. Hence, an attempt was done in this study to evaluate the effects of the particle angularity and surface roughness of the MS and blended sands on the workability of mortars from a linear regression analysis as represented in Figure 9. The results plotted are based on the performance of a typical mortar type. It can be observed that the angularity and surface roughness negatively affected the flow of fresh mortar with the R^2 values of 0.8764 and 0.8401, respectively.

The research carried out by Gonçalves et al. (2007) observed the declined consistency of mortars with the increasing sphericity of sand particles. As similar to the observations made in the present study, Yuli et al. (2011) also noticed that the increasing roughness of MS particles enhanced a declining trend with the flow of mortars. Some authors related the gradation of sand particles to the consistency of mortars. For example, Guifeng et al. (2014) identified that the decreasing fractions of smaller particles considerably increased the consistency of mortars.

4.1.3. Workable life

The freshly mixed mortars were undergone for the penetration resistance test to determine the workable life. Workable life is defined as the time elapsed between the preparation of mortars until the mortars remain in the plastic stage. During the masonry works, mortars must have enough workable life to enable the mason practitioners to carry out the works within the possible time.

As provided in Figure 10, the mean penetration resistance of S and N mortars were evolved with time. For both mortar types, RS mortars showed lower trends while the MS mortars were come up with inflated trends. It can be clearly observed that each variation of blended sand mortars lied between the RS and MS mortars. The variations were provided with linear trendlines and then interpolated for determining the corresponding workable life of mortars when the penetration resistance was 0.5 N/mm^2.

Figure 11 represents the mean workable life of each mortar obtained from the interpolation. The increasing MS content declined the workable life of mortars. The level of the effects of selected alternatives and the blending ratios on the workable life of mortars can be investigated from the ANOVA results.

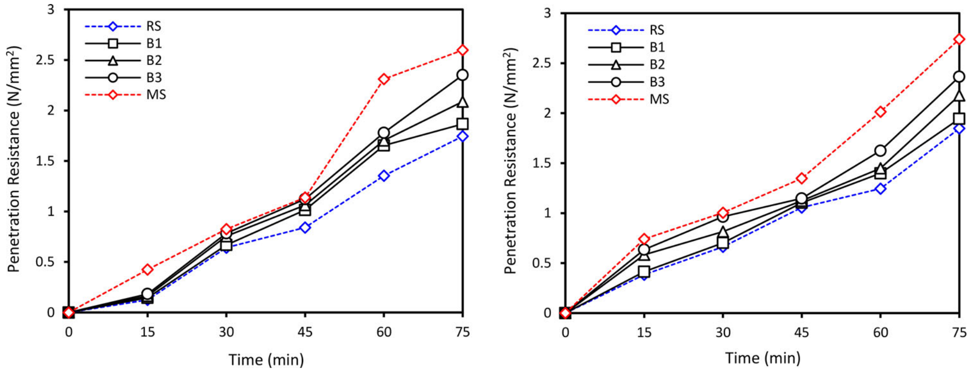

Figure 10. Variation of penetration resistance against time—S mortars (left) and N mortars (right).

Because the *p*-values of ANOVA were less than 0.05, the selected replacements of RS had a statistically significant effect on the workable life of S and N mortars at a 95% confidence interval. The observed *p*-values of S and N mortars are 0.002 and 0.0007, respectively.

The results from this investigation show the negative aspects of mortars incorporated MS and the blended sands. When considering the mortars prepared with MS alone, a significant decline was revealed than RS mortars. The OS inclusions as the MS replacements also did not improve this property than the control mortars. Similar results were observed in the studies by Ledesma et al. (2014) and Jiménez et al. (2013) where the authors found decreasing trends in the workable life when the RS in mortars were replaced with recycled concrete aggregates and ceramic wastes, respectively. Here, the effects of particle properties and gradation were not reported as the relationships were attained with very low R^2 values. Therefore, a future study is required on contemplating the most influencing parameters of fine aggregates that affect the workable life of masonry mortars.

4.1.4. Bleeding

Bleeding occurs in the fluid mortars when the sand particles suspended in the fresh cement paste tend to settle down due to the gravity force. This could lead to some serious issues in the mortars when the bled water rapidly evaporates from the surface. Generally, tension forces are created at the mortar surfaces after the evaporation of bled water, which ultimately results in shrinkage cracking.

Figure 12 illustrates the average cumulative bleeding of mortars after 1 hour from the casting. Based on the variations observed, the B1 mortars revealed a lower average cumulative bleeding than the RS mortars. However, all the other alternative mortars showed a gradually advancing trend. When comparing the MS and RS mortars of both types, MS mortars manifested a significantly higher cumulative bleeding than RS mortars. The rationale for this inflation is the sudden increase in the specific gravity of MS sand particles than the RS particles which could enhance a quick settlement owing to gravity.

This significance of the results can be statistically proved from the ANOVA test outcomes. The *p*-values of ANOVA were observed for S and N mortars as 3E-06 and 1E-05, respectively. Because the *p*-values were lower than 0.05, it was deduced that the RS replacements with MS and the blended sands had a statistically significant effect on the cumulative bleeding of mortars at a 95% confidence interval. Furthermore, it was identified that the selected particle properties and the packing density of sands did not affect this fresh property where significant correlations were not observed during the regression analysis.

4.1.5. Water retentivity

The capacity of retaining the water against external suction is a very important factor that needs to be investigated carefully for the fresh masonry mortars. Several studies proved that, when bricks or blocks used for the masonry works are in a dry state, then rapid suction could take place by the dried bricks or blocks at the mortar interface, which ultimately results in the lower strength and bonding capacity of mortars (Navaratnarajah & Rumeshkumar, 2018; Sahu et al., 2019).

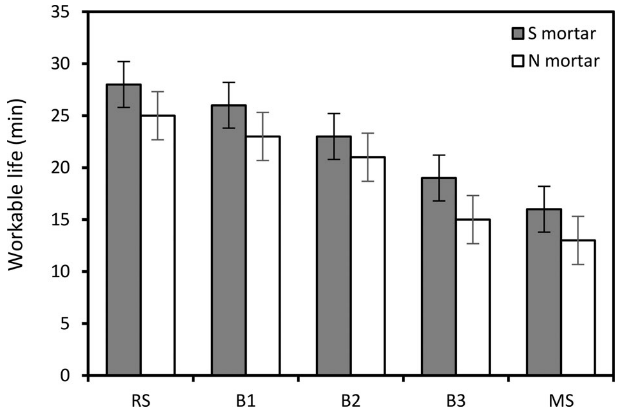

Figure 11. Effects of alternatives and blended sands on workable life of mortars.

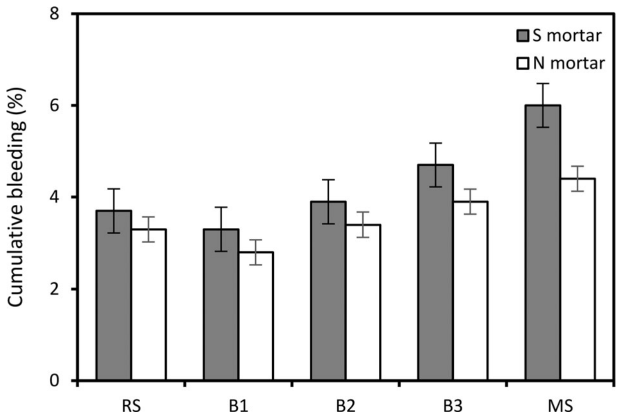

Figure 12. Effects of alternatives and blended sands on bleeding of mortars.

Figure 13 exhibits the average water retentivity of the mortars prepared in this work. The MS mortars showed decreased retention capacities than the RS mortars. This can be related to the particle size distribution of the selected sand types. As discussed above, RS revealed a uniform gradation while some particle size ranges of MS lied out of the standard permissible region. This may lead to variations in the penetrability of water through the pores present in fresh mortars. Furthermore, the blended sand mortars slightly improved the capacity against the suction of water than the MS mortars which may be due to the uniform gradations of the blended sands (refer Figure 2).

Because the *p*-values of ANOVA were lower than 0.05 (the obtained *p*-values were 0.001 and 0.0002 for the S and N mortars, respectively), the RS replacements with the selected alternatives and the blending ratios had a statistically significant effect on the water retentivity of mortars at a 95% confidence interval.

Due to the unavailability of parameters to correlate the gradation and the water retention capacity of mortars, the packing density of sand types was related to the water retentivity of mortars as illustrated in Figure 14. A polynomial correlation with an acceptable R^2 value of 0.5513 was observed between these properties. It also should be noted that the gradation curves provided in Figure 2 were derived for the particles above 0.075 mm. However, the micro fines in the selected sand types could also affect the test results due to the direct influence on the packing density of sand. Therefore, an extensive future study is required concerning these issues to find a more accurate correlation between the properties.

Few studies related different properties of fine aggregate with the water retentivity of mortar. Based on the studies implemented by Penacho et al. (2014) and Martínez et al. (2016), an increasing trend can be observed with the water retentivity of mortars when RS was replaced by fine glass waste and recycled concrete aggregates. The authors related the variations of specific surface properties of fine aggregates with the changes in the water retentivity of mortars.

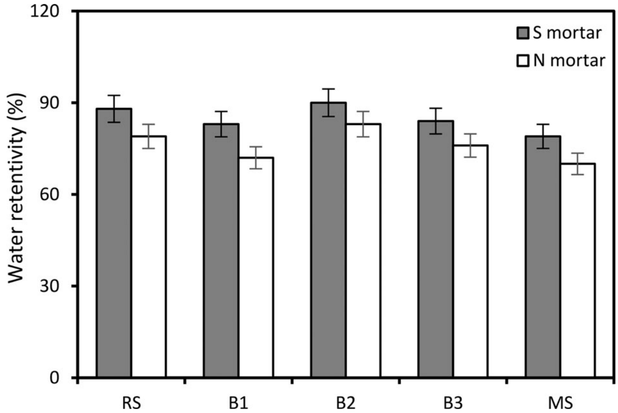

Figure 13. Effects of alternatives and blended sands on water retentivity of mortars.

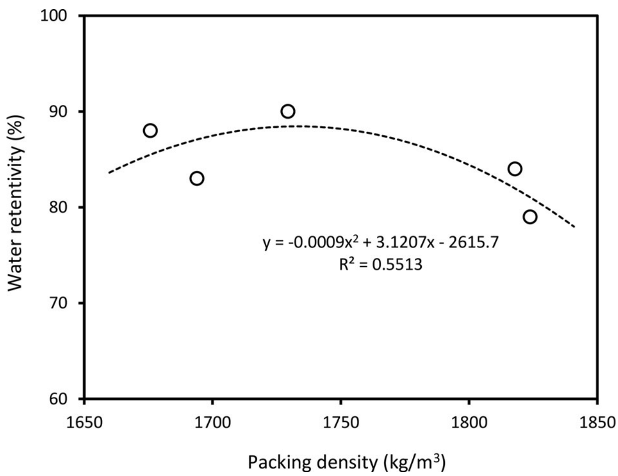

Figure 14. Relationships between water retentivity of mortars and the packing density.

4.1.6. Flexural and compressive strengths

The flexural and compressive strengths are considered the most critical mechanical characteristics of a mortar. The masonry mortars should have enough strength to resist the compressive and bending stresses generate in the masonry walls from the structural and wind loads. The strength of a mortar primary depends on the properties of aggregates that are incorporated. Therefore, this study determined the flexural and compressive strengths of mortars manufactured with the selected alternatives and the blending ratios at different curing ages according to the industrial requirements as shown in Figure 15.

The compressive strength of S and N mortars linearly increased with the MS contents at 2 and 28 days of curing. Similar trends were also noticed with the flexural strength test results at the selected curing ages. Moreover, a significant difference of strengths can be noticed between the MS mortars and RS mortars which was mainly due to the variation of particle properties. The combined particle effects of MS and OS also improved the strengths of blended sand mortars than the reference mortars.

The results of the statistical analysis are also reported here to determine the level of significance between the strengths of mortars. Because the *p*-values of ANOVA were less than 0.05 (the observed values are 3E-18 and 6E-14 for S and N mortars, respectively), the alternatives and blending ratios had a statistically significant effect on the 2 days compressive strength of mortars at 95% confidence interval. Regarding the 28 days compressive strength results, the *p*-values of ANOVA for S and N mortars were obtained as 3E-19 and 2E-12 which are lower than 0.05 at a 95% confidence interval. This also shows the statically significant effects of the selected mix designs on the 28 days compressive strength of mortars.

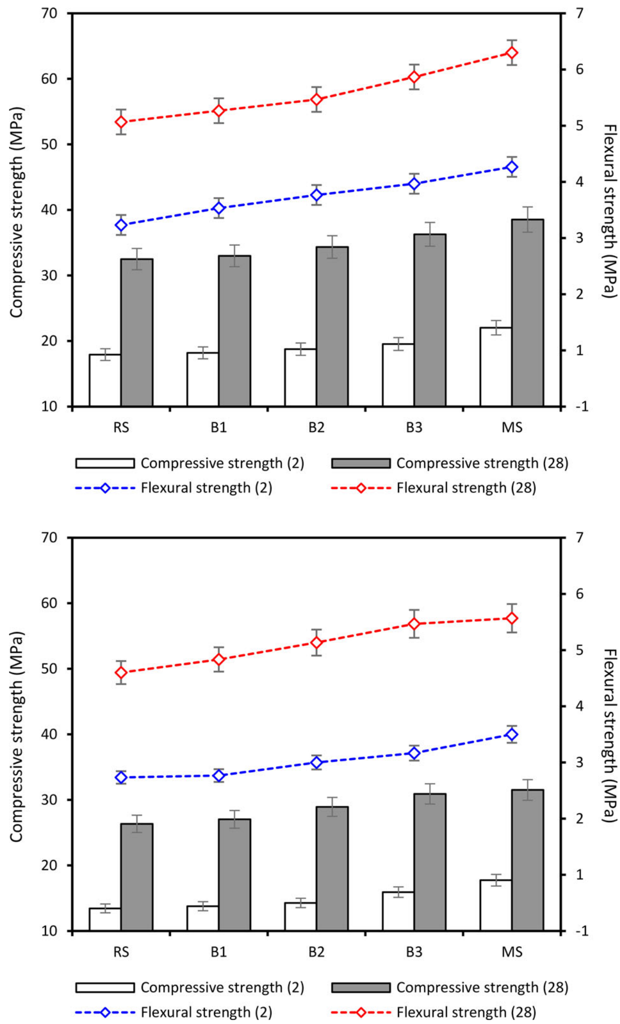

Figure 15. Effects of alternatives and blended sands on flexural and compressive strengths of S mortars (upper) and N mortars (lower) at 2, 28 days curing.

The selected alternatives and blending ratios also proved statistically significant effects on the 2- and 28-days flexural strength of mortars at 95% confidence interval. The observed *p*-values with the 2 days flexural strength results are 7E-06 and 4E-05 for S and N mortars, respectively. The *p*-values of the ANOVA test on the 28 days flexural strength results were determined as 3E-07 and 2E-07 for S and N mortars, respectively. Here, the null hypothesis can be rejected as each *p*-value is lower than 0.05.

The interlocking between the particle shapes and the frictional resistance between the particle surfaces are the dominant factors that could impact the strength of mortars. The angularity index and the surface roughness index of sands can be directly correlated to the compressive and flexural strengths of mortars. To determine the effects of particle properties on the strengths of mortars, regression analyses were carried out as illustrated in Figure 16.

A positive linear relationship can be noticed between the angularity index of sand particles and the strengths of mortars. Based on the R^2 values, a good linear correlation can be made between the angularity index of the sand types and the compressive strength (with $R^2 = 0.9300$) and flexural strength (with $R^2 = 0.9285$) of mortars. When concerning the relationship between the surface roughness index and the strengths of mortar, in both cases a positive polynomial trend was achieved with a good R^2 value (i.e., 0.9810 for compressive strength and 0.9987 for flexural strength of mortar).

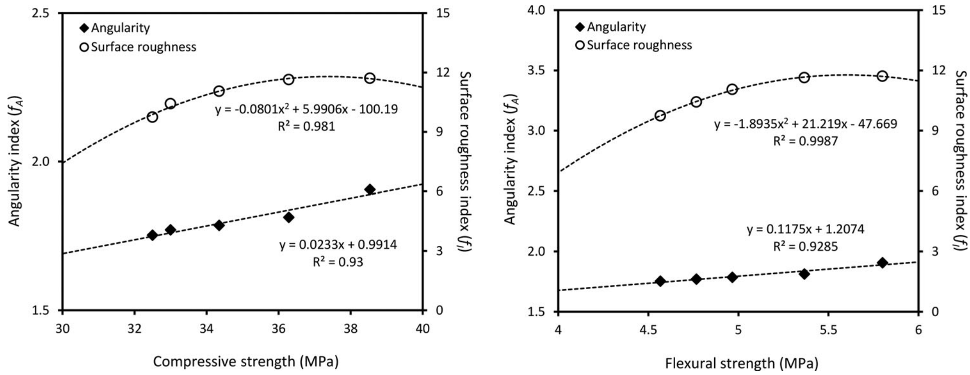

Figure 16. Relationships between the angularity and surface roughness indexes of particles and the compressive and flexural strengths of mortars.

Similar behavior as discussed above can be found from some previous studies implemented based on the performance of concrete. Li et al. (2011) and Shen et al. (2016) found a significant positive correlation between the particle shape and roughness of MS particles and the compressive and flexural strengths of pavement cement concrete and ordinary concrete, respectively. Bentz et al. (2017) also concluded the positive effects of angularity and surface roughness of different rock-derived aggregates on the strength characteristics of concrete. However, a clear correlation cannot be observed between the roughness index of aggregates and the compressive and split tensile strengths of concrete in the study executed by Poloju et al. (2017).

4.1.7. Linear shrinkage and thermal expansion

In this study, the dimensional stability was investigated when mortars were exposed to room temperature as well as the elevated temperature conditions. Linear shrinkage of mortars was tested up to 7 days from the casting day as a short-term study. However, the thermal expansion of mortars was evaluated after the mortars achieved stability against shrinkage. Figure 17 illustrates the variation of the average linear shrinkage of mortars incorporated the selected alternatives and the blending ratios.

As illustrated, the mortars comprised of MS alone revealed the highest linear shrinkage at each testing day. Comparing with RS mortars, the B2 and B3 mortars showed higher shrinkage while the B1 mortars manifested a lower shrinkage trend. These behaviors can be directly related to the effective water-to-cement ratios (w/c $_{ef}$) of the mortars as listed in Table 5. During the mixing of mortars, it was observed that the water demand was advanced with the increasing MS content. The absorption of water was considerably increased with the presence of micro-fine at higher MS levels due to the larger total specific surfaces. Moreover, as a result of the replacement of MS by OS, the water demand of blended sand mortars was slightly reduced which ended up in a lower shrinkage than MS mortars.

The results obtained in this work can be matched with the studies carried out by Ledesma et al. (2014) and Houria et al. (2020). The above authors utilized recycled concrete aggregates and marble waste sand, respectively as the partial replacements for RS in mortars. Both studies concluded the higher drying shrinkage of mortars with increased free-water contents. The study executed by Ferreira et al. (2011) reported that the shrinkage of concrete was improved when the recycled coarse concrete aggregates were included at the natural moisture without pre-saturated. Zega and Di Maio (2011) also found that the concrete produced with the same fine aggregate content and effect w/c ratios resulted in similar drying shrinkage.

Because the *p*-values of ANOVA were not less than 0.05 (the observed *p*-values are 0.89 and 0.87 for S and N mortars, respectively), RS replacements with the selected alternatives and the blending ratios did not prove statistically significant effects on the cumulative linear shrinkage of mortars up to 7 days from casting.

Figure 18 shows the average thermal expansion of mortars suspected to the elevated temperature for 24 hours. The results obtained here are contradicted by the observations made during the linear shrinkage of mortars. It can be identified that RS mortars manifested the highest expansion coefficients while

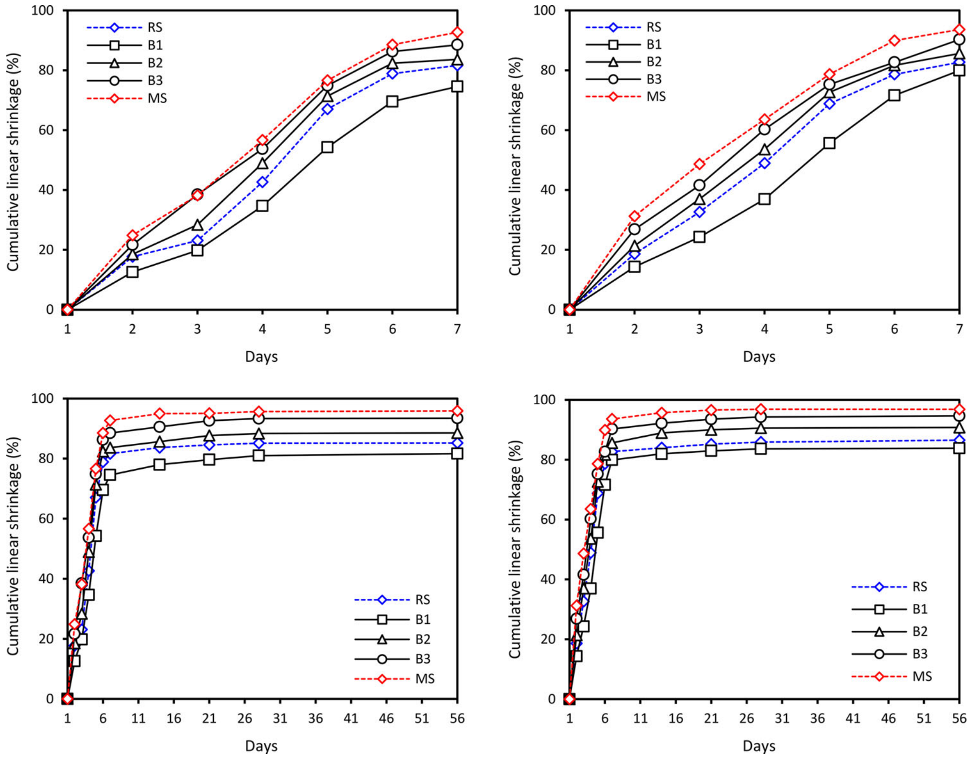

Figure 17. Effects of alternatives and blended sands on linear shrinkage of S mortars (left) and N mortars (right) at 7 and 56 days.

MS mortars revealed the lowest. A gradual decrease was observed with the blended sand mortars when the replacement of MS by OS was changed from 75% to 25%. Hence, the different behavior of the selected sand types could influence the experimental outcomes and a future study is mandatory on relating the above results with the thermal coefficient of each selected sand type.

Because the *p*-values of ANOVA were lower than 0.05 (the obtained *p*-values are 2.1E-09 and 1.5E-12 for S and N mortars, respectively), the selected RS alternatives and the blending ratios had a statistically significant effect on the thermal expansion of mortars at a 95% confidence interval.

4.1.8. Capillary water absorption

The determination of the capillary suction of hardened mortars was also carried out as a short-term study as stated in the corresponding standard. It is obvious that the rate of water absorption and the cumulative amount of water absorbed by stiffened mortar is mainly affected by the surface characteristics which is exposed to or contacted with water. Figure 19 represents the variations of the mean capillary water suction of hardened mortars measured at 24 hours from the immersion.

A significant variation was not observed with the cumulative water absorption of S and N mortars after 4 hours of immersion. This effect can be found in the long-term study executed by Stefanidou and Papayianni (2005). When contemplating the absorption of individual mortars, MS revealed the highest water absorption followed by the RS mortars. However, the blended sand mortars considerably declined the water absorptions at each interval. Based on the experiment results, the particle size distribution played a major role in the rate of absorption and the cumulative water suction. Table 8 can be referred for an extensive analysis on this which emphasizes the distribution of macro and micro pores presented in the contacted surface of representative mortars obtained through an image processing technique. Here, the sizes (area) pores were measured using the 'area' tool in the software and the pores were classified as 1–1.5 mm for macropores and <1 mm for micropores (Note that the classification was done as authors' wish).

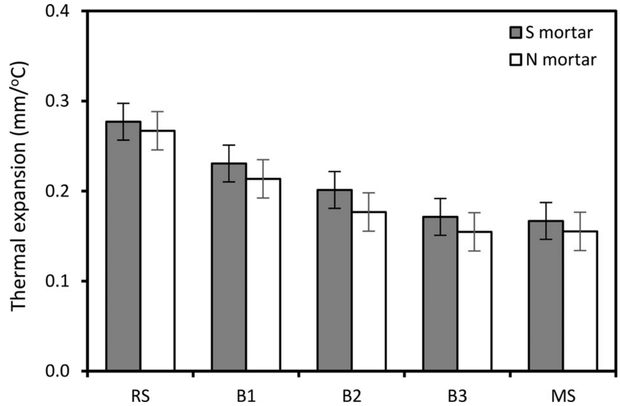

Figure 18. Effects of alternatives and blended sands on thermal expansion of mortars.

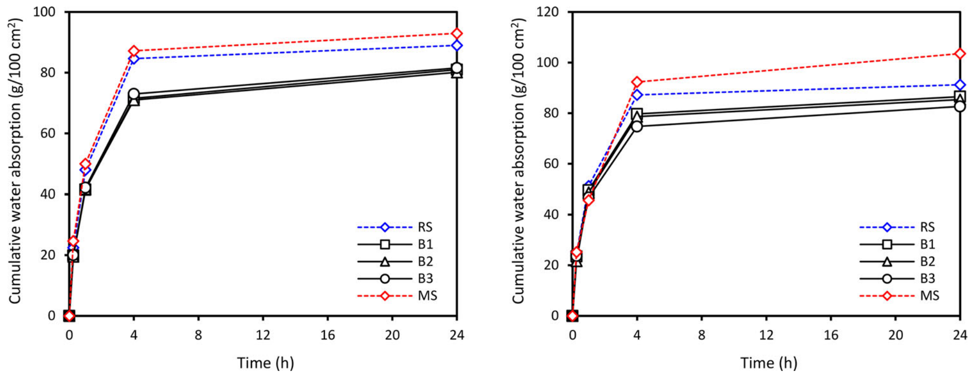

Figure 19. Effects of alternatives and blended sands on capillary water suction of S mortars (left) and N mortars (right).

As an initial step, the packing density of the sand types was related to the average cumulative water absorption of mortars at 24 hours from the immersion as plotted in Figure 20. However, no significant relationship was noticed between the above properties. It should be noted that a good positive correlation was observed between the total surface pore area obtained from the image processing technique and the cumulative capillary suction at 24 hours with an R^2 value of 0.9256. Hence, it can be concluded that the presence of pores in the contacted surface directly influenced the initial rate of water absorption by the mortars. Furthermore, to investigate the effects on the cumulative water absorption at 24 hours, this work should be extended by analyzing the presence of the internal pores created in the mortar specimens.

The work implemented by Gonçalves et al. (2007) also found a similar relationship between the water absorptivity and total porosity of mortars. The authors also observed that the absorptivity of mortars produced with the micro-fine removed MS was reduced than the RS mortars, which partially satisfies the future recommendation of the present work. Few studies evaluated the capillary water suction of mortars with different RS alternatives. Ledesma et al. (2014) and Neno et al. (2013) found the lower water absorption of mortars with increasing micro-fine content in recycled concrete aggregates. However, contradictory outcomes were noticed by the research carried out by Samiei et al. (2015) where the absorptivity of lime-cement mortars was diminished with increasing recycled concrete aggregates contents. Penacho et al. (2014) observed a perfect linear increasing relationship between the water absorption of mortar and the replacement of RS with glass waste, which was due to the higher total porosity at larger replacements.

The level of effects of the selected alternatives and blending ratios on the cumulative capillary water absorption of mortars at 24 hours from the immersion was checked from the ANOVA test. The *p*-values of ANOVA resulted as 1.6E-08 and 2E-10 for S and N mortars, respectively. Because the *p*-values were lower than 0.05, it can be deduced that RS replacements with the selected alternatives and blending

Table 8. Micro-images of the surface morphologies of mortars contacted with water (for a typical mortar type).

RS (114.526)	B1 (81.327)	B2 (85.632)
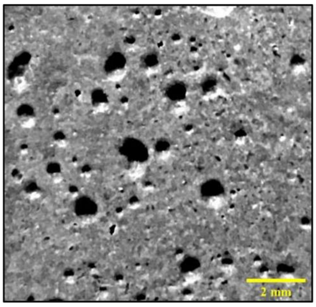	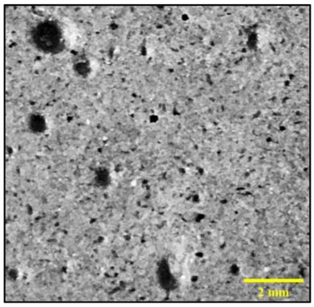	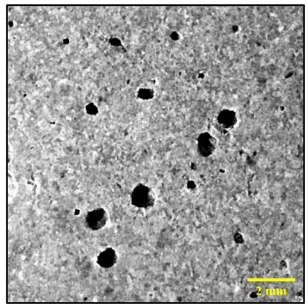
B3 (79.889)	MS (115.633)	
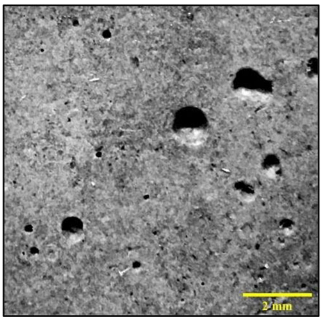	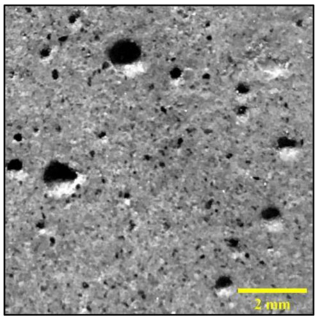	

Note. Value in parenthesis represents the total surface pore area (area of macropores + area of micropores) in mm^2.

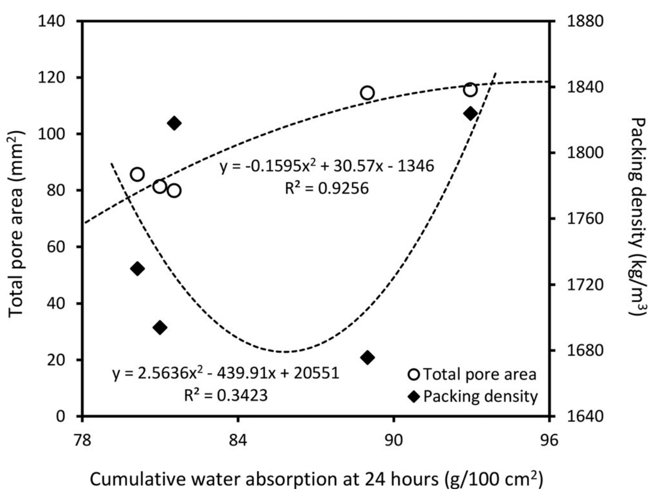

Figure 20. Relationships between the total pore area and packing density and the capillary water absorption of mortars at 24 hours.

ratios had a statistically significant effect on the cumulative capillary water absorption of mortars at a 95% confidence interval.

4.1.9. Alkali-silica reactivity

The alkali-silica reactivity (ASR) test was performed on the designed mortars as a long-term study. Figure 21 illustrates the variations of the linear expansion of mortars against time for each mortar when they

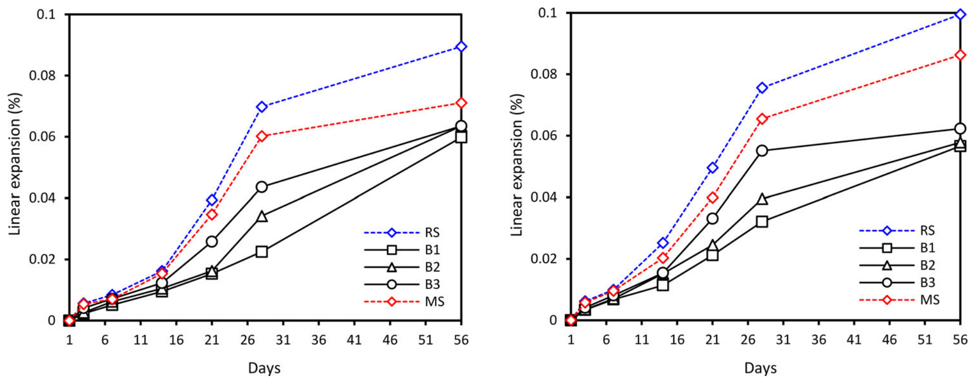

Figure 21. Effects of alternatives and blended sands on ASR induced expansion of S mortars (left) and N mortars (right).

were exposed to the NaOH environment. The results of ASR-induced expansion were obtained as the average of three identical mortar bars for each type.

Considering the expansions at 14 and 28 days, the S mortar incorporated RS alone manifested 0.0162% and 0.0698%, respectively. These values were noticed with the N mortar as 0.0252% and 0.0756%, respectively. A slightly reduced expansion than RS mortars were noted with the mortars that contained MS alone. The S mortars with MS alone revealed the expansions of 0.0154% and 0.0602% at 14 and 28 days. These observations were made with the N-MS mortar as 0.0203% and 0.0655%, respectively. Therefore, the full replacement of RS with MS could be able to reduce the vulnerability to the alkali-silica reaction. Regarding the mortars consisted of the selected blended sands, a distinct observation can be made where the rate of reactivity was considerably reduced than the RS and MS mortars of both mortar types. The partial replacement of MS with OS declined the alkali-silica reactivity, and this can be rationalized from the below consequences.

One of the basic factors that influence the alkali-silica reactivity is the permeability of the mix after hardened. The permeability of mortars (when different sand types are incorporated while keeping other constituents constant) depends on the density of sand as well as the porosity. Denser mixtures leading to the declined intrusion of the external alkalis by lowering the permeability. This could be able to reduce the alkali-silica gel that forms in the hardened mixes and the related damages (Bahedh & Jaafar, 2018; Graybeal, 2006).

When concerning the packing density of the fine aggregate types that are considered for this study, the blended sand mortars showed increased densities than RS. However, the MS revealed the highest packing density. Hence, the other factor that affected the alkali-silica reactivity is the porosity. As provided in Table 8, the total pore area was increased in the mortar specimens that contained RS and MS alone. This highlights the increased permeability of RS and MS mortars with the presence of higher macro and micropores. However, these pores were lowered in the blended sand mortars which reduced the permeability and the alkali-silica reactivity.

The level of effects of the selected alternatives and blending ratios on the cumulative ASR expansion of mortars at 56 days was determined from the ANOVA test. The p-values of ANOVA resulted as 0.7330 and 0.6190 for S and N mortars, respectively. Because the p-values were higher than 0.05, the selected alternatives and blending ratios did not show a statistically significant effect on ASR-induced expansion mortars at a 95% confidence interval.

4.2. Cost comparison of mortars with the RS replacements

The increased demand highlights the inflated market price index of RS. The industries are now facing many difficulties as they are spending more expenditure for consuming RS for the construction activities. Hence, this work reports the cost comparisons of the selected mortars to check whether the proposed alternatives and the blending ratios are acceptable for producing low-cost mortars.

To achieve the aim of this work, a cost comparison was carried out among each proposed mortar considering a particular mortar type. This was done to neglect the effects of the price indexes of other

Table 9. Comparison of the expenditure of mortars.

Mortar designation	Price index of mortar	Cost less than reference mortar (%)	Graphical representation
RS	x	—	
B1	0.69x	31%	
B2	0.64x	36%	
B3	0.58x	42%	
MS	0.53x	47%	

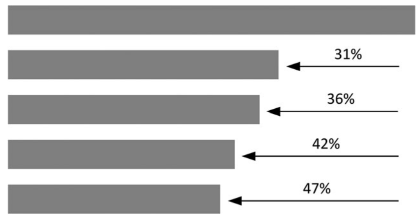

constituents utilized such as cement, lime, and water on the cost of mortar. Therefore, all the comparisons were only based on the price indexes of sand types.

The current market prices for 1 cube of RS, MS, and OS in Sri Lanka were obtained from the sand markets as 17,000, 9,000, and 12,500, respectively (in LKR) and then converted into an index method. For this analysis, initially, the market price of RS was converted into an index 'x' as a reference. Then the prefixes of 'x' for other sand types were determined according to the proportionality of the corresponding market prices. Therefore, the MS and OS were provided with the indexes of 0.53x and 0.74x, respectively. Table 9 lists the price index of each mortar and the percentage of deviation of alternative mortars from the reference mortar.

Among the selected sand types, RS showed an inflated market price while MS can be considered as the cheapest material. The price of OS lied between RS and MS. Because of the lowest market price of MS, the mortar produced with MS alone revealed 47% declined expenditure than the RS mortar. The blended sand mortars also manifested lower price indexes than the reference mortar due to the complete replacement of RS by MS and OS. The price indexes of blended sand mortars linearly decreased from 31% to 42% than RS mortar with the increasing MS content. Therefore, it can be concluded that each alternative mortar considered in this study is applicable for economical masonry constructions.

4.3. Summary of the experiment results, statistical analysis, and relationships derived

Table 10 shows a summary of the experimental results obtained in this study. Here, the numerical values of the properties of each mortar are the average from the selected number of specimens used for each test as mentioned in Table 6. It can be observed that most of the properties of fluid mortars incorporating MS alone and other blended sands such as B1, B2, and B3 were declined than the reference mortar. Few contradictory results were noticed with the workability, bleeding, and water retentivity of mortars for some replacements.

Regarding the hardened performance of mortars, RS replacements with the selected alternatives and the blending ratios proved satisfactory results with most of the properties except the linear shrinkage of mortars. However, it can be observed that the performance of mortar against capillary water absorption was declined when RS was replaced with MS alone. The durability of alternate mortars was also improved than control mortars which revealed reduced ASR induced expansions.

Except for the linear shrinkage and ASR of mortars, all the other experiment results evinced statistically significant effects with the replacement of RS in lime-cement mortars by MS alone and the blended sands comprised of MS and OS.

Table 11 describes the summary of the relationships derived with the acceptable coefficient of determination values (R^2) in this study between the property of mortars and the selected sand characteristics such as particle shape (angularity), particle surface roughness, and the particle size distribution (or packing density). It is clear that the particle properties such as the angularity and surface roughness mainly influenced the workability and strength properties of lime-cement mortars than other properties. Good correlations were noticed between the above properties with the high R^2 values. Hence, it can be concluded that the combined particle behavior of MS and OS also manifested an important role in the flowability and the strength of fresh and hardened lime-cement mortars.

Table 10. Summary of average test results and statistical analysis.

Experiment	Unit	Type	Average test results RS	B1	B2	B3	MS	*p*-value	OP	SS
Wet bulk density	[kg/m^3]	S	2292	2301▲	2316▲	2338▲	2396▲	6.1E-08	red	✓
		N	2255	2269▲	2275▲	2281▲	2341▲	1.0E-07	red	✓
Workability	[mm]	S	105	106▲	102▼	99▼	98▼	0.00015	orange	✓
		N	99	96▼	92▼	90▼	88▼	0.00013	red	✓
Consistency	[mm]	S	9.25	8.25▼	7.5▼	7.25▼	6.75▼	0.00317	red	✓
		N	7.75	7.5▼	6.75▼	7.25▼	5.25▼	0.00273	red	✓
Workable life	[min]	S	29	26▼	22▼	20▼	18▼	0.00225	red	✓
		N	27	24▼	22▼	16▼	15▼	0.00074	red	✓
Bleeding	[%]	S	3.7	3.3▼	3.9▲	4.7▲	6.0▲	3.0E-06	orange	✓
		N	3.3	2.8▼	3.4▲	3.9▲	4.4▲	1.0E-05	orange	✓
Water retentivity	[%]	S	88	82▼	89▲	83▼	77▼	0.001	orange	✓
		N	79	72▼	83▲	76▼	70▼	0.00168	orange	✓
Dry bulk density	[kg/m^3]	S	2047	2058▲	2074▲	2084▲	2098▲	1.6E-08	red	✓
		N	1825	1897▲	1945▲	2004▲	2024▲	5.0E-10	red	✓
Flexural strength	[MPa]	S (2)	2.7	3.0▲	3.3▲	3.5▲	3.8▲	7.2E-06	green	✓
		N (2)	2.2	2.3▲	2.5▲	2.7▲	3.0▲	3.5E-05	green	✓
		S (28)	4.6	4.8▲	5.0▲	5.4▲	5.8▲	3.2E-07	green	✓
		N (28)	4.1	4.3▲	4.6▲	5.0▲	5.1▲	2.0E-07	green	✓
Compressive strength	[MPa]	S (2)	17.9	18.2▲	18.8▲	19.6▲	22.0▲	2.6E-18	green	✓
		N (2)	13.5	13.8▲	14.3▲	15.9▲	17.6▲	6.5E-14	green	✓
		S (28)	32.5	33.0▲	34.4▲	36.3▲	38.5▲	3.0E-19	green	✓
		N (28)	26.4	27.0▲	28.9▲	30.9▲	31.5▲	2.4E-12	green	✓
Linear shrinkage	[%]	S (7)	81.6	74.6▼	82.4▲	88.5▲	92.7▲	0.89719	orange	✗
		N (7)	82.7	79.9▼	85.6▲	90.3▲	93.6▲	0.87387	orange	✗
Thermal expansion	[mm/°C]	S (28)	0.2770	0.2306▼	0.2013▼	0.1713▼	0.1668▼	2.1E-09	green	✓
		N (28)	0.2670	0.2136▼	0.1768▼	0.1547▼	0.1552▼	1.5E-12	green	✓
Capillary water absorption	[g/100 cm^2]	S (28)	89.0	81.0▼	80.1▼	81.5▼	93.0▲	1.6E-08	orange	✓
		N (28)	91.2	86.5▼	85.4▼	82.7▼	103.5▲	2.0E-10	orange	✓
ASR induced expasnion	[%]	S (56)	0.0895▼	0.0598▼	0.0635▼	0.0635▼	0.0711▼	0.7330	green	✗
		N (56)	0.0995▼	0.0566▼	0.0578▼	0.0623▼	0.0863▼	0.6190	green	✗

Note. OP = overall performance of mortar; SS = statistically significance of the effects of replacements;
▲, ▼ = results greater and lower than reference mortar (red and green defines the positive and negative effects, respectively).
red: Property was not improved with the alternative mortars.
orange: Property was partially improved with the alternative mortars.
green: Property was fully improved with the alternative mortars.

Table 11. Summary of the relationships.

Mortar property	Influencing parameter and R^2 value f_A	f_l	ρ_c	A	Relationship	Model
Workability (W)	0.8764				Polynomial [↘↗]	$f_A = 0.004\ W^2 - 0.76\ W + 41.27$
		0.8401			Linear [↘]	$f_l = -0.22\ W + 33.01$
Water retentivity (R)			0.5513		Polynomial [↗↘]	$R = -0.001\ \rho_c^2 + 3.12\ \rho_c - 2615.7$
Flexural strength (F_L)	0.9285				Linear [↗]	$f_A = 0.12\ F_L + 1.21$
		0.9987			Polynomial [↗]	$f_l = -1.89\ F_L^2 + 21.22\ F_L - 47.67$
Compressive strength (F_C)	0.9300				Linear [↗]	$f_A = 0.02\ F_C + 0.99$
		0.9810			Polynomial [↗]	$f_l = -0.08\ F_C^2 + 5.99\ F_C - 100.19$
Capillary water absorption ($\mathbb{C}$)				0.9256	Polynomial [↗]	$A = -0.16\ \mathbb{C}^2 + 30.57\ \mathbb{C} - 1346$
			0.3423		Polynomial [↘↗]	$\rho_c = 2.56\ \mathbb{C}^2 - 439.91\ \mathbb{C} + 20551$

Note. ↘ represents the negative trend (declining relationship); ↗ represents the positive trend (increasing relationship).

The water retentivity and capillary water absorption of lime-cement mortars were slightly affected by the packing density of selected alternatives and the blended sands. A remarkable relationship can be observed between the capillary water absorption of mortars and the total pore area presented in the surface of mortar specimens contacted with water. Here, concerning Table 8, the micro-images and the numerical values distinctly demonstrate a considerable reduction in the pores created when blended sands were introduced as a result of the good packing density. Furthermore, among the relationships derived in this work, most of them were identified with polynomial behavior while others revealed a linear relationship.

5. Conclusions

A novel concept of blending manufactured sand with offshore sand at different replacement levels such as 25%, 50%, and 75% was introduced in the present study for completely substituting river sand in lime-cement masonry mortars. The fresh state properties such as wet bulk density, consistency, and workable life were reduced for each alternate mortars comparing with the control mortar. Some improvements were identified in the workability, bleeding, and water retentivity of mortars which contained lower manufactured sand contents. The compressive and flexural strengths were increased in the range of around 40%–60% and 20%–30%, respectively than control mortars when blended sands were introduced. Higher stability against elevated temperature and lower water absorptions were also achieved with the replacements. The selected blended sands considerably advanced the durability of mortars where lower alkali-silica reactivity induced expansions were observed. Hence, the blended sand lime-cement mortars are effective in producing sustainable and economical masonry constructions.

Acknowledgement

The authors wish to thank the National Building Research Organization, Sri Lanka for providing supports for conducting the laboratory experiments, and INSEE Cement, Sri Lanka for granting required binding materials for this study.

Disclosure statement

No potential conflict of interest was reported by the authors.

ORCID

Branavan Arulmoly http://orcid.org/0000-0001-9058-6567

References

Aboutaleb, D., Safi, B., Chahour, K., & Belaid, A. (2017). Use of refractory bricks as sand replacement in self-compacting mortar. *Cogent Engineering*, *4*(1), 1360235. https://doi.org/10.1080/23311916.2017.1360235

Alshibli, K. A., & Alsaleh, M. I. (2004). Characterizing surface roughness and shape of sands using digital microscopy. *Journal of Computing in Civil Engineering*, *18*(1), 36–45. https://doi.org/10.1061/(ASCE)0887-3801(2004)18:1(36)

Aoual-Benslafa, F. K., Kerdal, D., Ameur, M., Mekerta, B., & Semcha, A. (2015). Durability of mortars made with dredged sediments. *Procedia Engineering*, *118*, 240–250. https://doi.org/10.1016/j.proeng.2015.08.423

Arulmoly, B., & Konthesingha, C. (2021). Pertinence of alternative fine aggregates for concrete and mortar: A brief review on river sand substitutions. *Australian Journal of Civil Engineering*. [Article in Press] https://doi.org/10.1080/14488353.2021.1971596

Arulmoly, B, Konthesingha, C, & Nanayakkara, A. (2021). Influence of Blended Fine Aggregates on the Performance of Lime - Cement Mortar – A Statistical Approach, 7th International Multidisciplinary Engineering Research Conference (MERCon 2021), IEEE, 27-29 July 2021. https://doi.org/10.1109/MERCon52712.2021.9525765

Arulmoly, B., Konthesingha, C., & Nanayakkara, A. (2021). Performance evaluation of cement mortar produced with manufactured sand and offshore sand as alternatives for river sand. *Construction and Building Materials*, *297*(7). https://doi.org/10.1016/j.conbuildmat.2021.123784

Arulmoly, B., Konthesingha, C., Nanayakkara, A., & Premasiri, R. (2021). Metamorphic Rocks for Manufactured Sand and Coarse Aggregate for Concrete and Mortar. *Magazine of Civil Engineering*, [Article in Press]. https://doi.org/10.34910/MCE.113.8

ASTM International. (1995). ASTM C117-95: Standard test method for materials finer than 75-✓m (No. 200) sieve in mineral aggregates by washing. In *Annual book of ASTM standards*. American Society for Testing and Materials.

ASTM International. (1997). ASTM C29/C29M-97: Standard test method for bulk density ("unit weight") and voids in aggregate. In *Annual book of ASTM standards*. American Society for Testing and Materials.

ASTM International. (2000a). ASTM C531-00 (reapproved 2012): Standard test method for linear shrinkage and coefficient of thermal expansion of chemical-resistant mortars, grouts, monolithic surfacings, and polymer concretes. In *Annual book of ASTM standards*. American Society for Testing and Materials.

ASTM International. (2000b). ASTM D3398-00: Standard test method for index of aggregate particle shape and texture. In *Annual book of ASTM standards*. American Society for Testing and Materials.

ASTM International. (2001). ASTM C128-01: Standard test method for density, relative density (specific gravity) and absorption of fine aggregate. In *Annual book of ASTM standards*. American Society for Testing and Materials.

ASTM International. (2003). ASTM C940-98a (reapproved 2003): Standard test method for expansion and bleeding of freshly mixed grouts for preplaced-aggregate concrete in the laboratory. In *Annual book of ASTM standards*. American Society for Testing and Materials.

ASTM International. (2006). ASTM C70-06: Standard test method for surface moisture in fine aggregate. In *Annual book of ASTM standards*. American Society for Testing and Materials.

ASTM International. (2010). ASTM C142/C142M: Standard test method for clay lumps and friable particles in aggregates. In *Annual book of ASTM standards*. American Society for Testing and Materials.

ASTM International. (2013). ASTM C1403-13: Standard test method for rate of water absorption of masonry mortars. In *Annual book of ASTM standards*. American Society for Testing and Materials.

ASTM International. (2017). ASTM C1506-17: Standard test method for water retention of hydraulic cement-based mortars and plasters. In *Annual Book of ASTM Standards*. American Society for Testing and Materials.

ASTM International. (2018a). ASTM C144-18: Standard specification for aggregate for masonry mortar. In *Annual book of ASTM standards*. American Society for Testing and Materials.

ASTM International. (2018b). ASTM C207-18: Standard specification for hydrated lime for masonry purposes. In *Annual book of ASTM standards*. American Society for Testing and Materials.

ASTM International. (2019a). ASTM C270-19ae1: Standard specification for mortar for unit masonry. In *Annual book of ASTM standards*. American Society for Testing and Materials.

ASTM International. (2019b). ASTM C294-19: Standard sescriptive nomenclature for constituents of concrete aggregates. In *Annual book of ASTM standards*. American Society for Testing and Materials.

ASTM International. (2021). ASTM C1260-21: Standard test method for potential alkali reactivity of aggregates (mortar-bar method). In *Annual book of ASTM standards*. American Society for Testing and Materials.

Bahedh, M. A., & Jaafar, M. S. (2018). Ultra high-performance concrete utilizing fly ash as cement replacement under autoclaving technique. *Case Studies in Construction Materials*, *9*, 1–9. https://doi.org/10.1016/j.cscm.2018.e00202

Balasubramanian, J., Gopal, E., & Periakaruppan, P. (2016). Strength and microstructure of mortar with sand substitutes. *Građevinar*, *68*(1), 29–37. https://doi.org/10.14256/jce.1245.2015

Bederina, M., Makhloufi, Z., Bounoua, A., Bouziani, T., & Quéneudec, M. (2013). Effect of partial and total replacement of siliceous river sand with limestone crushed sand on the durability of mortars exposed to chemical solutions. *Construction and Building Materials*, *47*, 146–158. https://doi.org/10.1016/j.conbuildmat.2013.05.037

Bentz, D. P., Arnold, J., Boisclair, M. J., Jones, S. Z., Rothfeld, P., Stutzman, P. E., Tanesi, J., Beyene, M., Kim, H., Munoz, J., & Ardani, A. (2017). Influence of aggregate characteristics on concrete performance. National Institute of Standards and Technology. https://doi.org/10.6028.NIST.TN.1963

Branavan, A., & Konthesingha, K. M. C. (2019). *Fine aggregate usage in concrete and masonry mortar by local construction industries*. 10th International Conference on Structural Engineering and Construction Management (ICSECM 2019), Kandy, Sri Lanka, pp. 106–113. http://icsecm.org/wp-content/uploads/2021/03/Proceeding_Volume-01.pdf

Branavan, A., Konthesingha, K. M. C., Nanayakkara, S. M. A., & Premasiri, H. M. R. (2020). Optimizing blending of manufactured sand with offshore sand based on physical and virtue characteristics. *Journal of Materials Science Research and Reviews*, *6*(3), 11–31. https://www.journaljmsrr.com/index.php/JMSRR/article/view/30156

British Standards Institution. (1992). *BS 882: Specification for aggregates from natural sources for concrete*. British Standards Institution.

British Standards Institution. (1997). *BS 5328: Concrete—Part 1. Guide to specifying concrete*. British Standards Institution.

British Standards Institution. (1999a). *EN 1015-4: Methods of test for mortar for masonry—Part 4: Determination of consistence of fresh mortar (by plunger penetration)*. British Standards Institution.
British Standards Institution. (1999b). *EN 1015-9: Methods of test for mortar for masonry—Part 9: Determination of workable life and correction time of fresh mortar*. British Standards Institution.
British Standards Institution. (2000). *EN 197-1: Cement—Part 1: Composition, specifications and conformity criteria for common cements*. British Standards Institution.
British Standards Institution. (2004). *EN 1015-3: Methods of test for mortar for masonry—Part 3: Determination of consistence of fresh mortar (by flow table)*. British Standards Institution.
British Standards Institution. (2007a). *EN 1015-6: Methods of test for mortar for masonry—Part 6: Determination of bulk density of fresh mortar*. British Standards Institution.
British Standards Institution. (2007b). *EN 1015-10: Methods of test for mortar for masonry—Part 10: Determination of dry bulk density of hardened mortar*. British Standards Institution.
British Standards Institution. (2007c). *EN 1015-11: Methods of test for mortar for masonry—Part 11: Determination of flexural and compressive strength of hardened mortar*. British Standards Institution.
British Standards Institution. (2015). *EN 459-1: Building lime. Definitions, specifications and conformity criteria*. British Standards Institution.
British Standards Institution. (2016). *BS EN 998-2: Specification for mortar for masonry. Masonry mortar*. British Standards Institution.
Chow, R. K. K., Yip, S. W. S., & Kwan, A. K. H. (2013). Processing crushed rock fine to produce manufactured sand for improving overall performance of concrete. *HKIE Transactions*, *20*(4), 240–249. https://doi.org/10.1080/1023697X.2013.861186
Cuffari, B. (2019). The applications of mortar in construction. Article ID: 8344, AZO Build [online]. Retrieved September 21, 2020, from https://www.azobuild.com/article.aspx?ArticleID=8344#:~:text=Bricklaying%20mortar%20is%20most%20commonly,the%20structure%20is%20being%20built
Dias, W. P. S., Seneviratne, G. A. P. S. N., & Nanayakkara, S. M. A. (2008). Offshore sand reinforced concrete. *Construction and Building Materials*, *22*, 1377–1384. https://doi.org/10.1016/j.conbuildmat.2007.04.006
Ferreira, L., Brito, J., & Barra, M. (2011). Influence of the pre-saturation of recycled coarse concrete aggregates on concrete properties. *Magazine of Concrete Research*, *63*(8), 617–627. https://doi.org/10.1680/macr.2011.63.8.617
Gavriletea, M. D. (2017). Environmental impacts of sand exploitation. Analysis of sand market. *Sustainability*, *9*(1118), 1–26. https://doi.org/10.3390/su9071118
Gonçalves, J. P., Tavares, L. M., Filho, R. D. T., Fairbairn, E. M. R., & Cunha, E. R. (2007). Comparison of natural and manufactured fine aggregates in cement mortars. *Cement and Concrete Research*, *37*, 924–932. https://doi.org/10.1016/j.cemconres.2007.03.009
Graybeal, B. A. (2006). Material property characterization of ultra-high performance concrete. US Department of Transportation [online]. Retrieved August 22, 2021, from https://www.fhwa.dot.gov/publications/research/infrastructure/structures/06103/06103.pdf
Guifeng, L., Shichao, L., Zhengfa, C., & Yanlong, Q. (2014). Effect of different grain grading of manufactured-sands on properties of dry-mixed mortar. *Trans Tech Publications*, *507*, 429–433. http:///doi.org/10.4028/www.scientific.net/AMM.507.429 https://doi.org/10.4028/www.scientific.net/AMM.507.429
Houria, H., Leila, K., Assia, A., & Mouloud, B. (2020). Introduction of marble waste sand in the composition of mortar. In *Sandy materials in civil engineering—Usage and management*. IntechOpen. https://doi.org/10.5772/intechopen.91254
ICTAD. (2004). ICTAD Publication No: SCA/4/1—Specifications for Building Works (Vol. I, 3rd ed., revised). Ministry of Housing and Construction.
Jaffe, R. C. (2001). Understanding mortar: Masonry materials. Article ID: M01B020, Hanley-Wood, LLC [online]. Retrieved October 17, 2020, from file:///C:/Users/User/Downloads/Concrete%20Construction%20Article%20PDF_%20Understanding%20Mortar_%20Masonry%20Materials.pdf
Jiménez, J. R., Ayuso, J., Lopéz, M., Fernandez, J. M., & de Brito, J. (2013). Use of fine recycled aggregates from ceramic waste in masonry mortar manufacturing. *Construction and Building Materials*, *40*, 679–690. https://doi.org/10.1016/j.conbuildmat.2012.11.036
Koehnken, L., Rintoul, M. S., Goichot, M., Tickner, D., Loftus, A.-C., & Acreman, M. C. (2020). Impacts of riverine sand mining on freshwater ecosystems: A review of the scientific evidence and guidance for future research. *River Research and Applications*, *36*, 362–370. https://doi.org/10.1002/rra.3586

Ledesma, E. F., Jiménez, J. R., Fernandez, J. M., Galvin, A. P., Agrela, F., & Barbudo, A. (2014). Properties of masonry mortars manufactured with fine recycled concrete aggregates. *Construction and Building Materials*, *71*, 289–298. https://doi.org/10.1016/j.conbuildmat.2014.08.080

Li, B., Ke, G., & Zhou, M. (2011). Influence of manufactured sand characteristics on strength and abrasion resistance of pavement cement concrete. *Construction and Building Materials*, *25*(10), 3849–3853. https://doi.org/10.1016/j.conbuildmat.2011.04.004

Limeir, J., Agulló, L., & Etxeberria, M. (2013). Dredged marine sand as construction material. *European Journal of Environmental and Civil Engineering*, *16*(8), 906–918. https://doi.org/10.1080/19648189.2012.676376

Martínez, I., Etxeberria, M., Pavón, W., & Díaz, N. (2016). Analysis of the properties of masonry mortars made with recycled fine aggregates for use as a new building material in Cuba. *Revista de la Construcción*, *15*(1), 9–21. https://doi.org/10.4067/S0718-915X2016000100001

Murdock, L. (1960). The workability of concrete. *Magazine of Concrete Research*, *12*(36), 135–144. https://doi.org/10.1680/macr.1960.12.36.135

Navaratnarajah, S., & Rumeshkumar, U. (2018). Effect of moisture condition on mechanical behavior of low strength brick masonry. *Journal of Building Engineering*, *17*, 23–31. https://doi.org/10.1016/j.jobe.2018.01.015

Neno, C., de Brito, J., & Veiga, R. (2013). Using fine recycled concrete aggregate for mortar production. *Materials Research*, *17*(1), 168–177. https://doi.org/10.1590/S1516-14392013005000164

Padmalal, D., Maya, K., Sreebha, S., & Sreeja, R. (2008). Environmental effects of river sand mining: a case from the river catchments of Vembanad lake, Southwest coast of India. *Environmental Geology*, *54*, 879–889. https://doi.org/10.1007/s00254-007-0870-z

Penacho, P., Brito, J., & Veiga, M. (2014). Physico-mechanical and performance characterization of mortars incorporating fine glass waste aggregate. *Cement & Concrete Composites*, *50*, 47–59. https://doi.org/10.1016/j.cemconcomp.2014.02.007

Pereira, K., & Ratnayake, R. (2013). Water integrity in action: Curbing illegal sand mining Sri Lanka. Water Integrity Network, Berlin [online]. Retrieved July 16, 2020, from http://www.waterintegritynetwork.net/wp-content/uploads/2015/04/Case_SriLanka_SandMining_EN_2013.pdf

Poloju, K. K., Anil, V., & Manchiryal, R. K. (2017). Properties of concrete as influenced by shape and texture of fine aggregate. *American Journal of Applied Scientific Research*, *3*(3), 28–36. https://doi.org/10.11648/j.ajasr.20170303.12

Radhakrishna, & Kumar, P. K. (2018). Characteristics of cement mortar with M-sand replacement of fine aggregates. *Materials Today: Proceedings*, *5*, 25412–25419. https://doi.org/10.1016/j.matpr.2018.10.346

Safi, B., Saidi, M., Aboutaleb, D., & Maallem, M. (2013). The use of plastic waste as fine aggregate in the self-compacting mortart: Effect on physical and mechanical properties. *Construction and Building Materials*, *43*, 436–442. https://doi.org/10.1016/j.conbuildmat.2013.02.049

Sahu, S., Teja, P. R. R., Sarkar, P., & Davis, R. (2019). Effect of brick prewetting on masonry bond strength. *Journal of Materials in Civil Engineering*, *31*(10), 1–9. https://doi.org/10.1061/(ASCE)MT.1943-5533.0002866

Samiei, R. R., Daniotti, B., Pelosato, R., & Dotelli, G. (2015). Properties of cement-lime mortars vs. cement mortars containing recycled concrete aggregates. *Construction and Building Materials*, *84*, 84–94. https://doi.org/10.1016/j.conbuildmat.2015.03.042

Shen, W., Yang, Z., Cao, L., Cao, L., Liu, Y., Yang, H., Lu, Z., & Bai, Y. (2016). Characterization of manufactured sand: Particle shape, surface texture and behavior in concrete. *Construction and Building Materials*, *114*, 595–601. https://doi.org/10.1016/j.conbuildmat.2016.03.201

Stefanidou, M., & Papayianni, I. (2005). The role of aggregates on the structure and properties of lime mortars. *Cement and Concrete Composites*, *27*, 914–919. https://doi.org/10.1016/j.cemconcomp.2005.05.001

Wigum, B. J., Danielsen, S. W., Hotvedt, O., & Pedersen, B. (2009). Production and utilisation of manufactured sand. SINTEF Building and Infrastructure, Oslo [online]. Retrieved June 18, 2020, from https://www.sintefbok.no/book/download/908/vinfopubutgivelserprosjektrapportcoin_project_reportscoin_report_no_12nettcoin-no12pdf

Yuli, W., Suxia, L., Weidong, W., & Yujie, Z. (2011). Influence of species of manufactured sand on basic performances of mortar. *Advanced Materials Research*, *306*, 980–983. https://doi.org/10.4028/www.scientific.net/AMR.306-307.980

Zega, C. J., & Di Maio, A. A. (2011). Use of recycled fine aggregate in concretes with durable requirements. *Waste Management*, *31*(11), 2336–2340. https://doi.org/10.1016/j.wasman.2011.06.011